Brazilian Journal
of Chemical
Engineering

ISSN 0104-6632
Printed in Brazil
www.abeq.org.br/bjche

Vol. 27, No. 04, pp. 653 - 662, October - December, 2010

ON BOUNDARY LAYER FLOW OF A DUSTY GAS FROM A HORIZONTAL CIRCULAR CYLINDER

Rebhi A. Damseh

Mechanical Engineering Department, Al-Huson University College,
Al-Balqa Applied University, P.O. Box 50, Irbid-Jordan,
Mob: 00962777495021, Fax: 009627010397
E-mail: Rdamseh@yahoo.com

(Submitted: October 12, 2009 ; Revised: January 15, 2010 ; Accepted: August 19, 2010)

Abstract - The problem of flow of a viscous incompressible gas with dust particles across an isothermal cylinder is discussed. The dust particles are assumed to be uniformly distributed throughout the gas. The equations of motion are simplified by writing the equations in dimensionless form and then solved numerically to describe the flow for different values of the physical parameters of interest. These parameters are the particle concentration parameter (R), the temperature relaxation time parameter (A) and the particle mass parameter (G). Many results are obtained and a representative set is displayed in graphs and tables. It is found that a distinct decrease in the velocity function is observed with an increase in the particle concentration parameter and increasing particle mass parameter induces a reduction in velocity. Furthermore, comparisons with previously published work are performed and the results are found to be in excellent agreement.
Keywords: Two-phase flow; Dusty gas-Horizontal cylinder; Heat transfer.

INTRODUCTION

Gas-particle flow, dusty fluid flow and the flow of suspensions have received considerable attention due to the importance of these types of flow in different engineering problems. The influence of dust particles on viscous flows has great importance in the petroleum industry and in the purification of crude oil. Other important applications of dust particles in the boundary layer include soil erosion by natural winds and dust entrainment in a cloud during a nuclear explosion. Also, such flows occur in a wide range of areas of technical importance like fluidization, flow in rocket tubes, combustion, paint spraying, and blood flow in capillaries.

Saffman (1962) discussed the stability of the laminar flow of a dusty gas in which the dust particles are uniformly distributed. Osiptsov (1997) reviewed the mathematical modeling of dusty-gas laminar boundary layers in the framework of the two-fluid approach. Formulation of the two-phase boundary layer approximation, using the matched asymptotic expansion method, was applied. The particle accumulation in the boundary layers and the effects of particles on the friction and heat fluxes were examined.

Dusty-gas flow in a laminar boundary layer over a body with a curved surface was considered by Asmolov (1995). An asymptotic approach was used; momentum equations for the particle phase were reduced to an algebraic equation accounting for the variation of lift coefficient with the shear and the slip velocity. Particle velocity and density were computed for the axisymmetric boundary layer in the neighbourhood of the front stagnation point of a blunt body. Samba Siva Rao (1969) obtained the analytical solutions for the dusty fluid flow through a circular tube under the influence of constant pressure gradient, using appropriate boundary conditions. Palani and Ganesan (2007) studied the heat transfer effects on dusty gas flow past a semi-infinite isothermal inclined plate. An implicit finite

*To whom correspondence should be addressed difference scheme was used to solve the non-dimensionalised governing boundary layer equations. Gas-velocity, dust particle-velocity, temperature, skin friction and Nusselt numbers were calculated numerically. Liu (1966) studied the flow induced by an oscillating infinite flat plate in a dusty gas. Michael and Miller (1966) investigated the motion of dusty gas with uniform distribution of the dust particles placed in the semi-infinite space above a rigid plane boundary. A model describing the flow of a dusty gas in porous media was developed in Hamdan and Barron (1990) and it is based on the differential equations approach. Dusty fluid flow through porous media with applications to deep filtration has been widely studied in Hamdan and Ford (1998) via an empirical and semi-empirical approach, the suggested model takes into account the optimal design of filters, liquid-dust separation and clogging mechanisms of the pores. In the case of flow of suspensions through a deep porous bed, Hamdan and Ford (1998) gave a review of the available literature and outlined the mechanisms of deposition and the possible capturing processes, which include sedimentation, inertial impacting, direct interception, hydrodynamic effects and diffusion by Brownian motion. Several researchers investigated the kinematical properties of fluid flows in the field of fluid mechanics like Truesdell (1960) and Indrasena (1978). Recently, Gireesha et al. (2006, 2007) studied the flow of an unsteady dusty fluid under several different pressure gradients like constant, periodic and exponential.

Much work has been done on the free and mixed convection boundary layer flow along a vertical and horizontal cylinder. Steady thermal convection studies for horizontal cylinders were reported by Sparrow and Lee (1977) and Ingham (1978). More recently Sadeghipour and Hannani (1992) considered the unsteady free convection from a horizontal cylinder between two vertical planes. Further studies of flow over cylindrical geometries have been presented by Kaminski et al. (1995), for the case of convective mass transfer by Sigwalt et al. (1996), and for the cases of a cavity and forced convection regimes by Cesini et al. (1999) and Karniadakis (1998). Heat and mass transfer in fluidized or packed beds of chemical reactors, as well as due to several possible mechanisms of mass transfer, are discussed from the point of view of applications of the present mathematical approach. Abbassi et al. (2002) considered the case of natural convection from elliptic cross-section cylinders. Sobera et al. (2004) studied the flow, heat, and mass transfer around a cylinder sheathed by a second, porous cylinder and placed in a perpendicular turbulent air flow, with applications in transport mechanisms in clothing in outdoor conditions.

The objective of this paper is to present numerical results for the problem of steady boundary layer flow of a dusty gas over a horizontal cylinder with uniform distribution of dust particles. Further, by considering that the fluid and dust particles are at rest initially, the boundary layer equations are transformed using non-similarity variables to a third order and a second order differential equation corresponding to the momentum and thermal equations. These equations are solved numerically using an implicit iterative tridiagonal finite-difference method. The effects of different physical parameters on the flow of dusty gas are shown graphically and presented in tabular form.

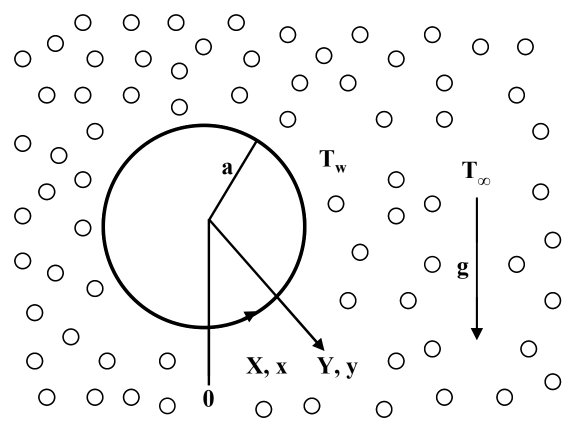

Figure 1: Geometry of the physical model

MATHEMATICAL FORMULATION AND SOLUTION

We investigate the free convective boundary layer flow of a dusty gas. We consider steady two-dimensional motion of incompressible heat and gas flow across an isothermal horizontal circular cylinder of radius a, Figure 1. The dust particles are assumed to be uniformly distributed throughout the gas and to be spherical in shape and uniform in size. Both the gas and the dust particle clouds are supposed to be static at the beginning. The number density of the dust particles is taken as a constant throughout the flow. Under these assumptions, the flow will be a parallel flow in which the streamlines are along the tangential direction and the velocities vary along the binormal direction, since we extended the fluid to infinity in the principal normal direction. The surface temperature of the cylinder is T_w and that of the ambient gas and the dust particles is assumed to be equal to T_∞, where $T_w > T_\infty$. The orthogonal coordinates X and Y are measured along the surface of the cylinder, starting with the lower stagnation point, and normal to it, respectively. Assuming constant thermophysical properties, under the Boussinesq approximation, the equations of motion of a viscous incompressible fluid with uniform distribution of dust particles are given by Saffman (1962):

For the fluid phase

$$\frac{\partial U}{\partial X}+\frac{\partial V}{\partial Y}=0 \tag{1}$$

$$\rho\left(U\frac{\partial U}{\partial X}+V\frac{\partial U}{\partial Y}\right)=\mu\frac{\partial^2 U}{\partial Y^2}+ \rho g\beta_T\left(T-T_\infty\right)\sin\left(\frac{X}{a}\right)+KN\left(U_p-U\right) \tag{2}$$

$$\rho\left(U\frac{\partial T}{\partial X}+V\frac{\partial T}{\partial Y}\right)=\frac{k}{c_p}\left(\frac{\partial^2 T}{\partial Y^2}\right)+\frac{\rho_p C_s}{\tau_T}\left(T_p-T\right) \tag{3}$$

For the dust phase

$$\frac{\partial U_p}{\partial X}+\frac{\partial V_p}{\partial Y}=0 \tag{4}$$

$$U_p\frac{\partial U_p}{\partial X}+V_p\frac{\partial U_p}{\partial Y}=\frac{K}{m_p}\left(U_p-U\right) \tag{5}$$

$$U_p\frac{\partial T_p}{\partial X}+V_p\frac{\partial T_p}{\partial Y}=-\frac{\left(T_p-T\right)}{\tau_T} \tag{6}$$

The appropriate boundary conditions for the problem are given by:

$$\begin{aligned}
&Y\le 0 \quad U=U_p=0 \quad T=T_p=T_\infty\\
&Y=0: \quad U=U_p=0 \quad V=V_p=0 \quad T=T_p=T_w\\
&Y\to\infty: U=U_p=0 \quad T=T_p=T_\infty
\end{aligned} \tag{7}$$

where ρ, μ are the density and viscosity of the clean fluid. U, U_p, V, V_p are the velocity components of fluid and dust particles along the X and Y axes. T, T_p are the temperature of the fluid and dust particles, respectively. N is the number density of dust particles, K = 6 π r μ is the Stoke's resistance (drag coefficient) and r is the spherical radius of the dust particles. m_p is the average mass of the dust particles, τ_T is the temperature relaxation time ($3\Pr\gamma_p C_s/2c$), which is the time taken by the dust particle to adjust to the motion of the fluid, γ_p is the velocity relaxation time, ($2\rho_s D^2/9\mu$) , ρ_s is the material density of the dust particles ($3\rho_p/4\pi D^3 N$), D is the average radius of the dust particles. k is the thermal conductivity, c_p is the specific heat at constant pressure. The last terms on the right –hand side of Equations (2) and (5) represent the heat conduction and the force due to the relative motion between the fluid and dust particles, respectively.

To solve Equations (1-7) the problem is simplified by writing the equations in dimensionless form. Thus we define the following non-dimensional quantities, Hye et al. (2007) and Attia (2005):

$$\begin{aligned}
&x=\frac{X}{a},\ y=\frac{Y}{a}Gr^{1/4},\ u=\frac{aU}{\nu Gr^{1/2}},\ v=\frac{aV}{\nu Gr^{1/4}},\\
&\theta=\frac{T-T_\infty}{T_w-T_\infty},\ Gr=\frac{g\beta_T\left(T_w-T_\infty\right)a^3}{\nu^2},\\
&\Pr=\frac{\mu c_p}{k},\ R=\frac{KNa^2}{\mu Gr^{1/2}},\ A=\frac{\tau_T KN}{\rho_s C_s\Delta T},\\
&G=\frac{m_p\mu Gr^{1/2}}{\rho a^2 K}
\end{aligned} \tag{8}$$

Implementation of the variables (8) in the boundary layer Equations (1) to (6) with the boundary conditions (7) leads to the following dimensionless partial differential equations:

$$\frac{\partial u}{\partial x}+\frac{\partial v}{\partial y}=0 \tag{9}$$

$$\left(u\frac{\partial u}{\partial x}+v\frac{\partial u}{\partial y}\right)=\frac{\partial^2 u}{\partial y^2}+\theta\sin(x)+R\left(u_p-u\right) \tag{10}$$

$$\left(u\frac{\partial \theta}{\partial x}+v\frac{\partial \theta}{\partial y}\right)=\frac{1}{\Pr}\left(\frac{\partial^2\theta}{\partial y^2}\right)+\frac{R}{A}\left(\theta_p-\theta\right) \tag{11}$$

$$\frac{\partial u_p}{\partial x}+\frac{\partial v_p}{\partial y}=0 \tag{12}$$

$$u_p\frac{\partial u_p}{\partial x}+V_p\frac{\partial u_p}{\partial y}=\frac{1}{G}\left(u_p-u\right) \tag{13}$$

$$u_p\frac{\partial \theta_p}{\partial x}+v_p\frac{\partial \theta_p}{\partial y}=-\frac{R}{AC_s}\left(\theta_p-\theta\right) \tag{14}$$

$$y \le 0 \quad u = u_p = 0 \quad \theta = \theta_p = 0$$

$$y = 0: \quad u = u_p = 0 \quad u = u_p = 0 \quad \theta = \theta_p = 1 \qquad (15)$$

$$y \to \infty: \; u = u_p = 0 \quad \theta = \theta_p = 0$$

where x, y are dimensionless coordinates along and normal to the tangent of the cylindrical curved surface, u, u_p, v, v_p, are the dimensionless velocities of the fluid and dust particles in the x, y directions. θ, θ_p is the dimensionless temperatures of the fluid and dust particles, Gr is the Grashof number, Pr is the prandtl number, R is the particle concentration parameter, A is the temperature relaxation time parameter, G is the particle mass parameter.

Now we define a stream function ψ and, using the Cauchy-Rirmann equations:

$$\psi = x f(x,y), \qquad u = \frac{\partial \psi}{\partial y}, \qquad v = -\frac{\partial \psi}{\partial y} \qquad (16)$$

the dimensionless Equations (9-15) now become:

$$\frac{\partial^3 f}{\partial y^3} + f\frac{\partial^2 f}{\partial y^2} - \left[\frac{\partial f}{\partial y}\right]^2 + \theta\frac{\sin(x)}{x} + R\left(\frac{\partial f_p}{\partial y} - \frac{\partial f}{\partial y}\right) = x\left[\frac{\partial f}{\partial y}\frac{\partial^2 f}{\partial y \partial x} - \frac{\partial f}{\partial x}\frac{\partial^2 f}{\partial y^2}\right] \qquad (17)$$

$$\frac{1}{Pr}\frac{\partial^2 \theta}{\partial y^2} + f\frac{\partial \theta}{\partial y} + \frac{R}{A}\left(\theta_p - \theta\right) = x\left[\frac{\partial f}{\partial y}\frac{\partial^2 f}{\partial y \partial x} - \frac{\partial f}{\partial x}\frac{\partial^2 f}{\partial y^2}\right] \qquad (18)$$

$$f_p\frac{\partial^2 f_p}{\partial y^2} - \left[\frac{\partial f_p}{\partial y}\right]^2 - \frac{1}{G}\left(\frac{\partial f_p}{\partial y} - \frac{\partial f}{\partial y}\right) = x\left[\frac{\partial f_p}{\partial y}\frac{\partial^2 f_p}{\partial y \partial x} - \frac{\partial f_p}{\partial x}\frac{\partial^2 f_p}{\partial y^2}\right] \qquad (19)$$

$$f_p\frac{\partial \theta_p}{\partial y} - \frac{R}{AC_s}\left(\theta_p - \theta\right) = x\left[\frac{\partial f_p}{\partial y}\frac{\partial^2 f_p}{\partial y \partial x} - \frac{\partial f_p}{\partial x}\frac{\partial^2 f_p}{\partial y^2}\right] \qquad (20)$$

$$\frac{\partial f}{\partial y}(x,0) = 0 = \frac{\partial f_p}{\partial y}(x,0),$$
$$f(x,0) = 0, \quad \theta(x,0) = 1 = \theta_p(x,0) \qquad (21)$$
$$\frac{\partial f}{\partial y}(x,\infty) = 0 = \frac{\partial f_p}{\partial y}(x,\infty), \; \theta(x,\infty) = 0 = \theta_p(x,\infty)$$

where f is the dimensionless stream function and the primes denote differentiations with respect to y. The non-similar two-point boundary value problem defined by Equations (17) to (21) is strongly nonlinear and an analytical solution is extremely difficult. Self similarity of the conservation equations is achieved when x ~ 0, which physically corresponds to the lower stagnation point of the cylinder. For such case, the transformed conservation equations of the present model with some simplifications can be reduced to simpler ordinary equations as reported by Nazar et al. (2004). The parameter, x, in fact defines the curvature of the cylinder. At the upper stagnation point, $x \sim \pi$. The local Nusselt number and local skin friction coefficient at the cylinder surface are defined, respectively, by the following equations:

$$Nu_x Gr^{1/4} = -\frac{\partial\theta(x,0) + \partial\theta_p(x,0)}{\partial y}, \qquad Cf_x Gr^{-1/4} = x\frac{\partial^2 f(x,0) + \partial^2 f_p(x,0)}{\partial y^2} \qquad (22)$$

The partial differential Equations (17-21) are solved numerically by using an implicit iterative tridiagonal finite-difference method, as described by Cebeci and Bradshaw (1984). In this method, any quantity g at point (x_n, y_j) is written as g_j^n. Quantities at the midpoints of grid segments are approximated to second order as:

$$g_j^{n-1/2} = \frac{1}{2}\left(g_j^n + g_j^{n-1}\right), \quad g_{j-1/2}^n = \frac{1}{2}\left(g_j^n + g_{j-1}^n\right) \qquad (23)$$

and the derivatives are approximated to second order as:

$$\left(\frac{\partial g}{\partial x}\right)_j^{n-1/2} = \Delta x^{-1}\left(g_j^n - g_j^{n-1}\right), \qquad (g')_{j-1/2}^n = \Delta y^{-1}\left(g_j^n - g_{j-1}^n\right) \qquad (24)$$

where g is any dependent variable and n and j are the node locations along the x and y directions, respectively. First, the third-order partial differential equation is converted into a first order equation by the substitutions $f' = s$, and $s' = w$; the difference equations that are to approximate the previous equations are obtained by averaging about the midpoint $\left(x_n, y_{j-1/2}\right)$ and those to approximate the resulting equations by averaging about

$\left(x_{n-1/2}, y_{j-1/2}\right)$. At each line of constant x, a system of algebraic equations is obtained. With the nonlinear terms evaluated at the previous iteration, the algebraic equations are solved iteratively. The same process is repeated for the next value of x and the problem is solved line by line until the desired x value is reached. A convergence criterion based on the relative difference between the current and previous iterations is employed. When this difference reaches 10^{-5}, the solution is assumed to have converged and the iterative process is terminated.

The effect of the grid size Δy and Δx and the edge of the boundary layer y_∞ on the solution have been examined. The results presented here are independent of the grid size and y_∞ at least up to the 4th decimal place. Note that the right-hand terms in both the momentum and energy equations, which reflect the effect of the nonsimilarity on the mixed convection heat, transfer problem under consideration.

RESULTS AND DISCUSSION

Representative results for the non-dimensional temperatures (θ, θ_p) and velocities (u, u_p) as a function of distance normal to the cylinder surface, at the upper stagnation point ($x = \pi$), for the effects of the particle concentration parameter (R), the temperature relaxation time parameter (A) and the particle mass parameter (G) are obtained for a value of the Prandtl number equal to 0.7, which represents air at 20 C^o. Additionally, we have computed the variation of the local skin friction coefficient (dimensionless surface shear stress, Cf_x) and Nusselt number (Nu_x) as a function of coordinate x, (i.e., curvature parameter) along the cylinder surface.

In order to verify the accuracy of the present method, the values of the local skin friction coefficient (Cf_x) and Nusselt number (Nu_x) for clear fluid flow (R = 0) and Prandtl number Pr =1 are compared with the solutions obtained by Merkin (1976) and also Nazar et al. (2002) for the forced convective, purely fluid version of the general model. The results are in complete agreement, as can be seen in Table 1. We are, therefore, confident that the present results are accurate. In Table 1, we note that, for the case without dust particles, there is a continuous decrease in Nusselt number, Nu_x, from the lower stagnation point (x ~0) around the curved surface of the cylinder to the upper stagnation point (x ~ π). The shear stress function, Cf_x, however, increases from x = 0 and peaks between $x = \pi/2$ and π/3, decreasing markedly thereafter toward the upper stagnation point.

The velocity and temperature profiles for the fluid and dust particles are shown in Figures 2 and 3, respectively, for the effects of the particle concentration parameter (R). A distinct decrease in the velocity function is observed with an increase in the particle concentration parameter, which in all cases decays from a maximum at the cylinder surface (y = 0) to zero in the free stream, i.e., at the exterior of the boundary layer. The decrease in velocity with an increase in the particle concentration parameter causes the boundary layer thickness to become narrower. Consequently, the results obtained here indicate that the velocity of the fluid particles is parallel to the velocity of the dust particles. The fluid, which is nearer to the axis of flow, moves with a greater velocity than the dust particles. This is because the fluid velocity is the source of the duct particle velocity. As such, the particle concentration parameter (R) can be seen to exert a significant influence on the momentum in the buoyant flow regime, since it decelerates the flow. The influence of the particle concentration parameter (R) on the temperature profiles is to increase the temperature field. In turn, this causes the thermal boundary layer to increase and the temperature at every point also will increase, as shown in Figure 3. The fluid point temperature is higher than the dust particle temperature, which is consistent with the Equations 11 and 14. Thus, the source of heat for the dust particles is the fluid temperature.

Table 1: Values of the local Nusselt number Nu_x and skin friction coefficient Cf_x as a function of the curvature parameter x for R = 0, Pr = 1.0

	Nu_x			Cf_x		
x	Merkin (24)	Nazar et al (25)	Present method	Merkin (24)	Nazar et al (25)	Present method
0	0.4214	0.4214	0.4223	0.0	0.0	0.0
π/6	0.4161	0.4161	0.4158	0.4151	0.4148	0.4142
π/3	0.4007	0.4005	0.4008	0.7558	0.7542	0.7536
π/2	0.3745	0.3741	0.3745	0.9579	0.9545	0.9555
2π/3	0.3364	0.3355	0.3356	0.9756	0.9698	0.9663
5π/6	0.2825	0.2811	0.2816	0.7822	0.7740	0.7743
π	0.1945	0.1916	0.1922	0.3391	0.3265	0.3258

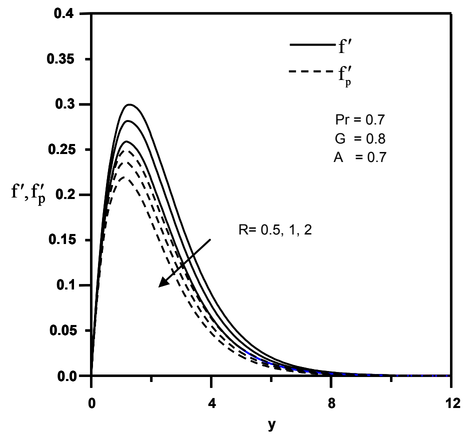

Figure 2: Fluid and dust velocities f', f_p' versus y for various values of the particle concentration parameter R

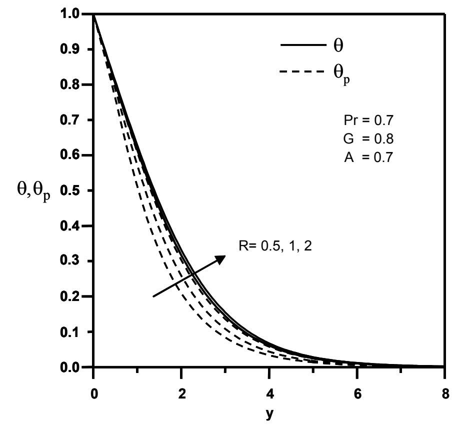

Figure 3: Fluid and dust temperatures θ, θ_p versus y for various values of the particle concentration parameter R

In Figure 4, the effect of the particle mass parameter (G) on the velocity field (f', f_p') for Pr = 0.7 is presented. The velocity peaks near to the cylinder surface for all values of R and then decays steadily to zero in the free stream. The presence of the peak indicates that the maximum value of the velocity occurs in the body of the fluid close to the surface and not at the surface. Increasing the particle mass parameter (G) induces a reduction in velocity, i.e., retards the flow, especially in the dust particle domain, irrespective of the value of any of the other parameters. Figure 5 shows that the fluid and dust point temperatures (θ, θ_p) increase notably with increasing particle mass parameter (G), a trend maintained throughout the boundary layer. This confirms earlier computations that indicated that the particle mass parameter (G) decelerates the flow and physically heats the fluid, albeit slightly.

The effect of the temperature relaxation time parameter (A) on the velocity and temperature profiles for the fluid and dust particles is shown in Figures 6 and 7. Physically, the temperature relaxation time is the time required by the dust particles to adjust to the motion of the fluid. As expected, higher values of the temperature relaxation time parameter (A) slightly affect the dust and fluid velocity profiles. In fact, a distinct increase in the velocity function f', f_p' is observed with an increase in the relaxation time parameter. The fluid point temperature increases noticeably as the relaxation time parameter (A) increases, Figure 7, but the dust-phase is not in syncrony with the fluid phase and requires more time. This results in a tendency to slow down the heat transfer process from the fluid to the dust particles, the reason for the decrease in the dust particle temperature.

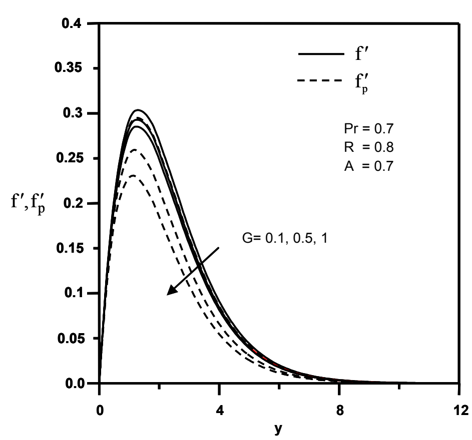

Figure 4: Fluid and dust velocities f', f_p' versus y for various values of the particle mass parameter G

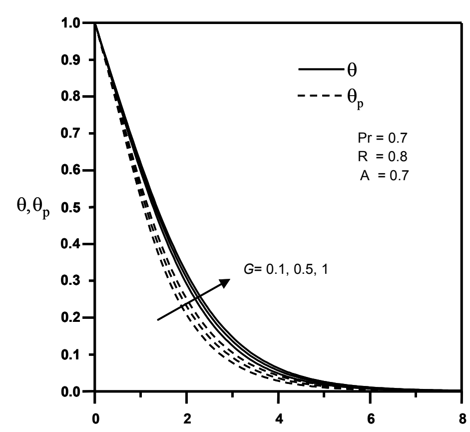

Figure 5: Fluid and dust temperatures θ, θ_p versus y for various values of the particle mass parameter G

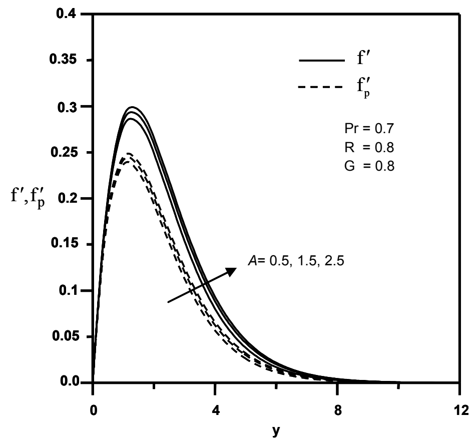

Figure 6: Fluid and dust velocities f', f_p' versus y for various values of the temperature relaxation time parameter A

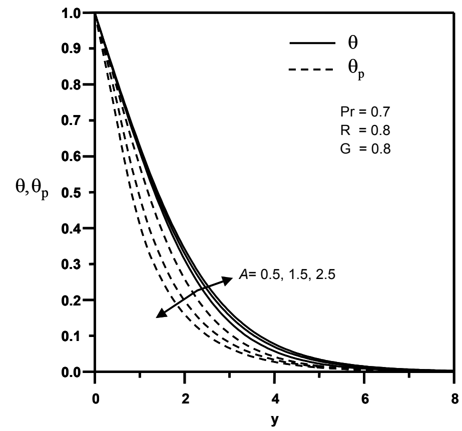

Figure 7: Fluid and dust temperatures θ, θ_p versus y for various values of the temperature relaxation time parameter A

In Figure 8, the variation of the local Nusselt number Nu_x for various values of the particle concentration parameter (R) is shown. The local Nusselt number Nu_x, defined by Equation (22), accounts for heat transfer in both the fluid and dust particles phases. Increasing R from 0.5 through 1, 1.5 to 3 (strong particle concentration) is seen to reduce the Nu_x values markedly, which decrease steadily from a peak at the lower stagnation point (x ~0) around the cylinder semi-circular surface to the upper stagnation point (x ~ π), where they are minimized. The values remain approximately the same at the upper stagnation point (x ~ π). The variation of the local surface shear stress function, Cf_x with the curvature parameter, i.e., the x coordinate along the curved surface, and the particle concentration parameter (R) is shown in Figure 9. Shear stress is seen to increase from the lower stagnation point (x ~0) towards the edge of the horizontal diameter (x ~ π/2), peaking before this point is reached at x ~ 1.4 and thereafter falling steadily towards the upper stagnation point (x ~ π). All profiles are parabolic and, with an increase in the particle concentration parameter (R), are reduced. As such, the effect of the particle concentration parameter (R) is to reduce shear stress values, which fall from a peak value of 1.6769 for R = 0.5 to 1.5025 for R = 3. The particle concentration parameter therefore decelerates the flow at the cylinder surface.

The variation of the local sheer stress function Cf_x and the local Nusselt number Nu_x with the x coordinate for different values of the particle mass parameter (G) and the temperature relaxation time parameter (A) are presented in Tables 2 and 3. It is imperative to notice here that all the calculations reflect the same behavior of the local Nusselt number and local sheer stress, as indicated in Figures 8 and 9. It can be seen from these tables that the values of Nu_x decrease as the particle mass parameter is increased and, conversely, increase with increasing values of the temperature relaxation time parameter. A similar effect on the local sheer stress function Cf_x is perceptible. This well-known relationship between the two physical functions, i.e., local sheer stress and local Nusselt number is addressed extensively in the literature.

Table 2: Values of the Local Nusselt number Nu_x and skin friction coefficient Cf_x as a function of the curvature parameter x for particle mass parameters G = 0.5, 1, 1.5 and fixed values of the particle concentration parameter (R = 0.8) and the temperature relaxation time parameter (A = 0.6).

x	$\frac{Nu_x}{Gr^{1/4}}$				$\frac{Cf_x}{Gr^{-1/4}}$			
	G=0.5	G =1	G =1.5	G =2	G =0.5	G =1	G =1.5	G =2
0	0.94153	0.91543	0.89625	0.88117	0	0	0	0
π/6	0.92879	0.90324	0.88444	0.86963	0.75149	0.72948	0.71063	0.69425
π/3	0.89089	0.86681	0.84906	0.83504	1.35175	1.31392	1.28146	1.25307
π/2	0.82813	0.80612	0.78978	0.776915	1.67107	1.62758	1.59036	1.55757
2π/3	0.75331	0.73007	0.71317	0.70000	1.61769	1.57916	1.54669	1.51807
5π/6	0.60617	0.58965	0.57712	0.56705	1.13744	1.11213	1.09153	1.07376
π	0.18155	0.19481	0.19444	0.19413	1.1698E-2	1.1563E-2	1.1439E-2	1.1324E-2

Table 3: Values of the Local Nusselt number Nu_x and skin friction coefficient Cf_x as a function of the curvature parameter x for temperature relaxation time parameters A = 0.5, 1.5, 2.5, 5 and fixed values of the particle concentration parameter (R = 0.8) and the particle mass parameter G = 0.8

x	$\frac{Nu_x}{Gr^{1/4}}$				$\frac{Cf_x}{Gr^{-1/4}}$			
	A=0.5	A=1.5	A=2.5	A=5	A=0.5	A=1.5	A=2.5	A=5
0	0.91925	1.03275	1.24632	1.82938	0	0	0	0
π/6	0.90736	1.01223	1.21531	1.78368	0.73673	0.74670	0.75423	0.76610
π/3	0.87175	0.95257	1.12418	1.64521	1.32638	1.34357	1.35679	1.37812
π/2	0.81193	0.85955	0.97988	1.41092	1.64190	1.66147	1.67703	1.70313
2π/3	0.73652	0.74083	0.79778	1.08167	1.59189	1.60819	1.62180	1.64614
5π/6	0.59563	0.59593	0.60449	0.68546	1.12065	1.12906	1.13660	1.15153
π	0.19495	0.19512	0.18140	0.18140	1.1616E-2	1.1615E-2	1.1616E-2	1.1614E-2

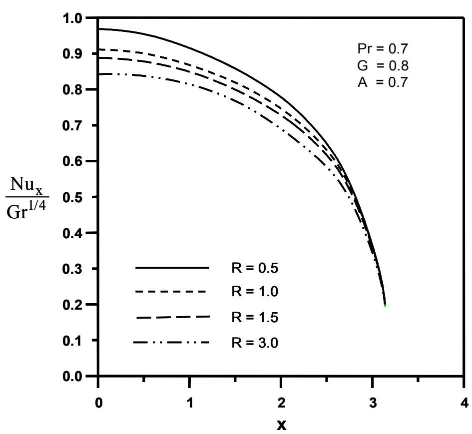

Figure 8: Local Nusselt number Nu_x versus x for various values of the particle concentration parameter R

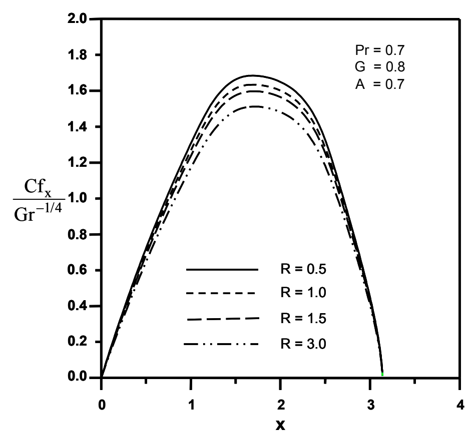

Figure 9: Local skin friction coefficient Cf_x versus x for various values of the particle concentration parameter R

CONCLUSIONS

The present study deals with a mathematical model for steady, two-dimensional free convection heat transfer of a dusty gas from an isothermal horizontal cylinder. The mathematical model developed incorporates the effects of the particle concentration parameter (R) and the particle mass parameter (G).

It is concluded that the velocity of fuid particles is parallel to the velocity of the dust particles. The fuid and dust particles that are nearer to the axis of flow, move with the greatest velocity. It was found that the influence of the particle concentration parameter (R) and the particle mass parameter (G) is to cause a decrease in the velocity function and an increase in the temperature field for both the fluid and dust phases. As a result, the presence of dust particles reduces the shear stress values. Simultaneously, this reduces the Nusselt number values. It is observed that the values of Nu_x decrease as the particle mass parameter increases and, conversely, increase with increasing values of the temperature relaxation time parameter (A). A similar effect on the local sheer stress function Cf_x is perceptible.

NOMENCLATURE

A	Temperature relaxation time parameter	
C_p	Specific heat of the fluid at constant pressure	J/kg K
C_f	Dimensionless surface shear stress	
g	magnitude of the acceleration due to gravity	m/s^2
G	Particle mass parameter.	
Gr	Grashof number	
K	Stoke's resistance	N.s/m
k	Thermal conductivity	W/m K
m_p	Average mass of the dust particles	kg

N	Number density of dust particles	
N_u	Nusselt number	
Pr	Prandtl number	
R	Particle concentration parameter	
T	Temperature of fluid	K
T_p	Temperature of dust particles	K
U, V	Fluid-phase velocity	m/s
U_p Vp	Particle-phase velocity	m/s
u, u_p	Dimensionless velocities of fluid and dust particles in the x direction	
v, v_p	Dimensionless velocities of fluid and dust particles in the y direction	
X, Y	Axial and transverse coordinates	m
x, y	Dimensionless axial and transverse coordinates	

Greek Symbols

β_T	Coefficient of thermal expansion	1/K
θ	Dimensionless temperatures of the fluid	
θ_p	Dimensionless temperature of the dust particles	
τ_T	Temperature relaxation time	s
μ	Dynamic viscosity	N.s/m^2
ρ	Fluid density	kg/m^3
ρ_p	Particle density	kg/m^3

Subscripts

∞	Free stream condition
w	Condition at the wall
x	Curvature parameter

REFERENCES

Abbassi, A., Basirat-Tabrizi, H., Nazemzadeh, S. A., Numerical analysis of steady –state laminar free convection over a horizontal cylinder with elliptic cross section, Progress in Transport Phenomena, Eds. S. Dost , H. Struchtrup and I. Dincer, 37-41, Elsevier (2002).

Asmolov, E. S., Dusty-gas flow in a laminar boundary layer over a blunt body. Journal of Fluid Mechanics, 305, p. 29 (1995).

Attia, H. A., Unsteady flow of a dusty conducting fluid between parallel porous plates with temperature dependent viscosity. Turk J, Phys., 29, p. 257 (2005).

Cebeci, T. and Bradshaw, P., Physical and Computational Aspects of Convective Heat Transfer. Springer, New York (1984).

Cesini, G., Paroncini, M., Cortella, G., Manzan, M., Natural convection from a horizontal cylinder in a rectangular cavity. Int. J. Heat and Mass Transfer, 42, p. 1801 (1999).

Gireesha, B. J., Bagewadi, C. S., Prasannakumara, B. C., Flow of unsteady dusty fluid under varying periodic pressure gradient. Journal of Analysis and Computation, 2, p. 183 (2006).

Gireesha, B. J., Bagewadi, C. S., Prasannakumara, B. C., Flow of unsteady dusty fluid under varying pulsatile pressure gradient in anholonomic co-ordinate system. Electronic Journal of Theoretical Physics, 4, no. 14, p. 9 (2007).

Hamdan, M. H., Barron, R. M., A dusty gas flow model in porous media. Comput. Applied Math., 30, p. 12 (1990).

Hamdan, M. A., Ford, R. A. R., Numerical simulation of gas particulate flow through curvilinear porous channels. J. Appl. Math. Comput., 4, p. 267 (1998).

Hye, M. A., Molla, M. A. and Khan, M. A. H., Conjugate effects of heat and mass transfer on natural convection flow across an isothermal horizontal circular cylinder with chemical reaction. Nonlinear Analysis: Modelling and Control J., 12, no. 2, p. 191 (2007).

Indrasena, A., Steady rotating hydrodynamic-flows. Tensor N. S., 32, p. 350 (1978).

Ingham, D. B., Free convection boundary layer on an isothermal horizontal cylinder. Z. Angew. Math. Phys (ZAMP), 29, p. 871 (1978).

Kaminski, D., Fu, X., Jensen, M., Numerical and experimental analysis of combined convective and radiative heat transfer in laminar flow over a circular cylinder. Int. J. Heat and Mass Transfer, 38, p. 3161 (1995).

Karniadakis, G., Numerical simulation of forced convection heat transfer from a cylinder in crossflow. Int. J. Heat and Mass Transfer, 31, no. 1, p. 107 (1998).

Liu, J. T. C., Flow induced by an oscillating infinite flat plate in a dusty gas. Phys. Fluids, 9, p. 1716 (1966).

Merkin, J. H., Free convection boundary layer on an isothermal horizontal cylinder. ASME/AIChemE Heat Transfer Conference, August 9-11, St. Louis, Missouri, USA (1976).

Michael, D. H., Miller, D. A., Plane parallel flow of a dusty gas, Mathematika, 13 p. 97 (1966).
Nazar, R., Amin, N. and Pop, I., Free convection boundary layer flow on an isothermal horizontal cylinder in a micropolar fluid. Proc. 12th Int. Heat Transfer Conference, Genoble, France, 2, 525-530 (2002).
Nazar, R., Amin, N., Pop, I., Mixed convection boundary layer flow from a horizontal circular cylinder in a micropolar fluid: case of constant wall heat flux. In. J. of Fluid Mechanics Research, 31, no. 2, p. 109 (2004).
Osiptsov AN, Mathematical modeling of dusty-gas boundary layer. Appl. Mech. Rev., 50, no. 6, p. 357 (1997).
Palani, G., Ganesan, P., Heat transfer effects on dusty gas flow past a semi-infinite inclined plate. Forschung im Ingenieurwesen, 70, no.3-4, p. 223 (2007).
Sadeghipour, M., Hannani, S., Transient natural convection from a horizontal cylinder confined between vertical walls – a finite element solution. Int. J. Numerical Methods in Engineering, 34, p. 621 (1992).
Saffman, P. G., On the stability of laminar flow of a dusty gas. Journal of Fluid Mechanics, 13, p. 120 (1962).
Samba Siva Rao, P., Unsteady flow of a dusty viscous liquid through circular cylinder. Def. Sci. J., 19, p. 135 (1969).
Sigwalt, P., Moreau M., Masure M., Xuanke L., Qingtian L., Hyung J.S., Jung S.Y. and Tae S.P., Local convective mass transfer on circular cylinder with transverse annular fins in crossflow, Int. J. Heat Mass Transfer, 39, No. 5, p. 1093 (1996).
Sobera, M. P., Kleijn, C. R., Van den Akker, H. E. A. and Brasser, P., Convective heat and mass transfer to a cylinder sheathed by a porous layer. AIChE J., 49, no. 12, p. 3018 (2004).
Sparrow, E.M. and Lee, L., Analysis of mixed, forced and free convection about a horizontal cylinder, Int. J. Heat Mass Transfer, 19, p. 229 (1977).
Truesdell, C., Intrinsic equations of spatial gas flows. Z. Angew. Math. Mech., 40, p. 9 (1960).